










RESEARCH PAPER



Exploring the activity of polyamine analogues on polyamine and spermine oxidase: methoctramine, a potent and selective inhibitor of polyamine oxidase

Maria Luisa Di Paolo^a , Manuela Cervelli^b , Paolo Mariottini^b , Alessia Leonetti^b , Fabio Polticelli^{b,c} , Michela Rosini^d , Andrea Milelli^e , Filippo Basagni^d, Rina Venerando^a, Enzo Agostinelli^{f,g}  and Anna Minarini^d 

^aDepartment of Molecular Medicine, University of Padova, Padova, Italy; ^bDepartment of Sciences, University of Roma Tre, Roma, Italy; ^cRoma Tre Section, National Institute of Nuclear Physics, Roma, Italy; ^dDepartment of Pharmacy and Biotechnology, Alma Mater Studiorum-University of Bologna, Bologna, Italy; ^eDepartment for Life Quality Studies, Alma Mater Studiorum-University of Bologna, Rimini, Italy; ^fDepartment of Biochemical Science "A. Rossi Fanelli", University of Rome "La Sapienza", Rome, Italy; ^gInternational Polyamines Foundation – ONLUS –Via del Forte Tiburtino 98, Rome, Italy

ABSTRACT

Fourteen polyamine analogues, asymmetric or symmetric substituted spermine (1–9) or methoctramine (10–14) analogues, were evaluated as potential inhibitors or substrates of two enzymes of the polyamine catabolic pathway, spermine oxidase (SMOX) and acetylpolyamine oxidase (PAOX). Compound 2 turned out to be the best substrate for PAOX, having the highest affinity and catalytic efficiency with respect to its physiological substrates. Methoctramine (10), a well-known muscarinic M₂ receptor antagonist, emerged as the most potent competitive PAOX inhibitor known so far ($K_i = 10$ nM), endowed with very good selectivity compared with SMOX ($K_i = 1.2 \mu\text{M}$ vs SMOX). The efficacy of methoctramine in inhibiting PAOX activity was confirmed in the HT22 cell line. Methoctramine is a very promising tool in the design of drugs targeting the polyamine catabolism pathway, both to understand the physio-pathological role of PAOX vs SMOX and for pharmacological applications, being the polyamine pathway involved in various pathologies.

ARTICLE HISTORY

Received 27 December 2018
Revised 6 February 2019
Accepted 14 February 2019

KEYWORDS

Polyamine analogues; docking studies; spermine oxidase; polyamine oxidase; inhibitors

Introduction

Polyamine (PA) metabolism plays an important role in cellular homeostasis, and its dysregulation may contribute to the development of several pathological states, including cancer^{1,2}. Elevated concentrations of polyamines have been associated with various types of tumours³; an increase in PA catabolism reaction products, which are reactive oxygen species and aldehydes (such as acrolein), has been implicated in causing cytotoxicity and in the pathogenesis of various diseases, such as liver and neurological disorders, and stroke^{4–11}. For these reasons, the PA metabolic pathway has been considered as a rational target for therapeutic approaches^{1,12–18}. To develop anti-cancer drugs, several PA analogues were designed to 'hit' some of the many players of this complex pathway.

To reduce the naturally occurring PA availability in cancer cells, some of the developed analogues targeting the biosynthetic pathway are, for instance, difluoromethyl-ornithine, which inhibits ornithine decarboxylase (ODC), the rate-limiting enzyme in the synthetic pathway^{1,3,18}, methylglyoxal(bis)guanyldiazide, which targets S-adenosylmethionine decarboxylase^{1,3,18} and the spermine (SPM) derivative named AMXT1501, which blocks the activity of polyamine transporters, avoiding the uptake of exogenous PA¹⁸. In the last years, the PA catabolic pathway is also emerging as a promising target for chemoprevention^{1,18–20}. In addition to

spermidine/spermine *N*¹-acetyltransferase (SSAT), two other key enzymes of this pathway are acetylpolyamine oxidase (PAOX) and spermine oxidase (SMOX), which are H₂O₂ producers. PAOX and SMOX, FAD-containing amine oxidases, have been biochemically characterised in a wide variety of organisms, including vertebrates, invertebrates and yeast^{8,21–23}. PAOX is a constitutively expressed enzyme and its preferred substrates are *N*¹-acetylspermine (*N*¹AcSPM) and *N*¹-acetylspermidine²⁴, whereas SMOX is an inducible enzyme specific for SPM⁸ and is highly expressed in some tissues, such as brain and skeletal muscle^{25–27}. Recently, in addition to the cytoplasmic and nuclear SMOX isoforms, SMOX activity was detected also in mitochondria²⁸. SMOX expression is increased in some type of cancers, it is induced by some bacterial infections and inflammatory cytokines, and by some PA analogues, such as *N*¹,*N*¹¹-bis(ethyl)norspermine (BenSPM)^{1,8,20,29–31}. In each case, the induction of SMOX is linked to an increase of H₂O₂ production and DNA damage, which correlates with the risk of developing dysplasia/cancer^{18,20}. In addition, epigenetic factors have been recently involved in the link between increased SMOX expression and carcinogenesis³².

On this basis, the availability of selective SMOX vs PAOX inhibitors would be of great value to develop chemopreventive agents. Furthermore, the selective inhibition of SMOX and PAOX, could allow for better understanding of the involvement of PA

CONTACT Maria Luisa Di Paolo  marialuisa.dipaolo@unipd.it  Department of Molecular Medicine, University of Padova, Via G. Colombo 3, 35131 Padova, Italy; Anna Minarini  anna.minarini@unibo.it  Department of Pharmacy and Biotechnology, Alma Mater Studiorum-University of Bologna, Via Belmeloro 6, 40126 Bologna, Italy

© 2019 The Author(s). Published by Informa UK Limited, trading as Taylor & Francis Group.

This is an Open Access article distributed under the terms of the Creative Commons Attribution-NonCommercial License (<http://creativecommons.org/licenses/by-nc/4.0/>), which permits unrestricted non-commercial use, distribution, and reproduction in any medium, provided the original work is properly cited.

catabolism in modulating tumorigenesis and the mechanism through which some PA analogues exert their anticancer activity.

Unfortunately, most of the mammalian PAOX and SMOX inhibitors currently available, suffer from poor selectivity, and overcoming this problem still remains an important goal for the development of novel pharmacological tools. SMOX and PAOX inhibitors are generally PA analogues³³, such as the irreversible and “well-known” MDL 72527 (*N*1,*N*⁴-bis(2,3-butadienyl)-1,4-butanediamine)³⁴ ($K_i=20$ and $63\ \mu\text{M}$, for purified murine PAOX and SMOX respectively)³³ and other butadienyl-spermidine derivatives with improved potency with respect to MDL 72527³⁵. Interestingly, some guanidine-containing derivatives have also shown promising inhibitory activity towards PAOX and SMOX. They include *N*-prenylagmatine (G3)³³, which has emerged as a good and selective competitive murine PAOX inhibitor ($K_i=0.8\ \mu\text{M}$ for PAOX and $K_i=46\ \mu\text{M}$ for SMOX), and iminoctadine (also known as guazatine), as a good but non-selective murine SMOX and PAOX inhibitor ($K_i \approx 0.5\ \mu\text{M}$). Recently, the antiseptic agent chlorhexidine has also been reported to act as a competitive inhibitor of murine PAOX and SMOX³⁶.

Three-dimensional crystal structures of enzymes may be of great support in designing and developing more selective SMOX or PAOX inhibitors. Unfortunately, in the case of mammalian enzymes, the crystal structure of murine PAOX³⁷ has been solved at present, while only molecular models are available for mammalian SMOX^{38,39}. Previous site-directed mutation studies have indicated that the aminoacids Leu195 and Ala197 in the active site of PAOX (Glu216 and Ser218 in SMOX) may be important in determining the different substrate specificity between PAOX and SMOX. The SMOX E216L/S218A mutant, in which Glu216 and Ser218 are mutated into PAOX orthologous residues, can oxidise *N*¹AcSPM in addition to SPM⁴⁰. However, this experimental result is not easy to explain on the basis of PAOX three-dimensional structures³⁷, which were obtained in complex with *N*¹AcSPM at pH 5.5, to maintain the oxidised state of FAD, and at pH 8 to obtain the reduced state of FAD, after its reaction with the substrate.

The murine PAOX crystal structure³⁷ revealed the very flexible nature of the protein and an L-shaped active site channel with a hydrophobic cavity in the interface between the domains adjacent to the family-invariant and catalytically relevant Lys315^{38,41,42}. The PAOX residue Asn313 (Thr in SMOX) plays an important role in the interaction with the acetyl group of *N*¹AcSPM through hydrogen bond formation. His64 also appears to be important in the interaction with the N5 (deprotonated form) of *N*¹Ac SPM; Asp211 interacts with both the side-chain of His64 and the backbone of Gly65, maintaining the overall structure of the enzyme. PAOX has an active site ideal for binding PAs, and the hydrophobic portion of the active site, which hosts the *N*¹-acetyl group of the substrate, should be able to accommodate large groups allowing van der Waals interactions with the surrounding residues.

In this context, structure-activity relationship studies with novel PA analogues may reveal information about the key features of molecules which give rise to selectivity between PAOX and SMOX.

In this study, SPM (1–9) and methoctramine (10–14) analogues^{43,44}, differing in the polyamine backbone and in the aromatic rings on the terminal nitrogen atoms, were used as probes to search for the optimal molecular features of PA analogues responsible for selective interactions with PAOX or SMOX. By means of a kinetic approach, the compounds were screened first as potential substrates and those inactive as substrates were tested as potential inhibitors. Methoctramine emerged as a potent and very selective PAOX inhibitor. Kinetic results were integrated

with docking simulations and the effectiveness of the most potent PAOX inhibitor was validated on a cellular model.

Materials and methods

Materials and instrumentations

All chemicals were of analytical-grade and purchased from Fluka-Aldrich S.r.l. (Milan, Italy) with the exception of Amplex Red reagent (10-acetyl-3,7-dihydroxyphenoxazine), purchased from Molecular Probes/Invitrogen (Invitrogen s.r.l., San Giuliano Milanese, Italy). Horseradish peroxidase, polyclonal anti-PAOX antibodies produced in rabbit and secondary antibodies (HRP-labelled anti-rabbit IgG) were purchased from Sigma-Aldrich S.r.l. (Italy).

The protein concentrations of the samples were determined according to the method of Bradford⁴⁵, with bovine serum albumin as standard protein. Stock solutions of the assayed compounds were prepared in water, with the exception of compound **6**, which was dissolved in dimethyl sulphoxide, and compounds **8** and **9**, dissolved in chloroform/methanol (1/1 v/v). A Cary-Eclipse fluorimeter (Varian Inc., Palo Alto, CA, USA) and a Cary 50 Scan UV-visible spectrophotometer (Varian Inc.) were used for fluorescence and spectrophotometric measurements, respectively.

PA analogues were synthesised as previously reported (compounds **1**, **8** and **9** in Bonaiuto et al.⁴⁶; compounds **2–7** in Bonaiuto et al.⁴⁷; methoctramine derivatives **10–12** in Melchiorre et al.⁴⁸, and Minarini et al.⁴⁹; compound **13** in Tumiatti et al.⁵⁰; compound **14** in Melchiorre et al.⁵¹).

Expression and purification of PAOX and SMOX proteins in *E. coli* cells

The recombinant PAOX and SMOX proteins were expressed in *E. coli* BL21 DE3 cells and purified according to Bianchi et al.³³ and Cervelli et al.²⁵, respectively. Purified recombinant proteins were analysed by SDS/PAGE electrophoresis to assess the grade of purity. Protein concentration was measured by the 460-nm molar extinction coefficient ($\epsilon_{460}=9000\ \text{M}^{-1}\ \text{cm}^{-1}$) which accounts for FAD absorption.

Amine oxidase activity assay

Amine oxidase activity was determined by measuring the H_2O_2 generation rate with a peroxidase-coupled continuous assay. Amplex Red reagent was used as fluorogenic substrate for horseradish peroxidase⁵². All experiments were carried out in Hepes 50 mM, at pH 7.5 and 37 °C. Phosphate buffer was not used, in order to avoid the possible formation of phosphate-SPM derivative complexes⁵³. Assays were carried out in a final volume of 800 μl , in the presence of Amplex Red (100 μM) and horseradish peroxidase type II (5 U/ml). The assay solutions containing SMOX or PAOX were pre-incubated for 2 min (in the presence or absence of the various compounds); the substrate was then added and the reaction was run continuously for 3 min. Spermine and *N*¹AcSPM were used as substrates for SMOX and PAOX, respectively. Enzyme assay concentrations were 0.5 $\mu\text{g}/\text{ml}$ and 0.3 $\mu\text{g}/\text{ml}$ for PAOX and SMOX respectively, unless otherwise specified.

Initial velocities were determined by measuring the increase in fluorescence intensity ($\lambda_{\text{exc}}=563\ \text{nm}$ and $\lambda_{\text{em}}=586\ \text{nm}$) over time; H_2O_2 generation rate was calculated from the change in fluorescence intensity, by means of calibration curves obtained by serial dilution of a stock solution of H_2O_2 . For each measurement, the corresponding blank, measured in the absence of the substrate,

was subtracted. No significant interference of the various compounds was observed on fluorescence intensity.

Docking simulations

Docking simulations were performed with the recently solved crystal structure of PAOX (PDB ID: 5LFO³⁷). The three-dimensional structure of small molecule ligands was built with Schrödinger Maestro 10.1 (Schrödinger, LLC, New York, NY, 2015). As literature data indicate that PAs bind within the PAOX active site in tri-protonated form⁴², the atomic charges of the ligands in this form were calculated with the AtomicChargeCalculator web server⁵⁴. Simulations were carried out with AutoDock Vina⁵⁵. In all simulations, to carry out “blind” predictions of small-molecule binding sites, the search space (docking grid) included the whole PAOX structure. The grid spacing was set to 1 Å per grid unit, and the exhaustiveness parameter was increased from the default value of 8–24, as suggested by Autodock Vina developers for grid sizes larger than 27,000 Å³ (see <http://vina.scripps.edu/tutorial.html>).

Simulations were carried out by allowing the flexibility of the residues to build the walls of the PAOX active sites, i.e. His61, Trp62, His64, Glu184, Cys186, Val187, Ser188, Phe201, Tyr204, Asn313, Lys315, Ile358, Phe375, Tyr430, Tyr472, Ser473 and Thr474. The rotatable bonds of the ligands were kept flexible in all simulations.

Cell cultures and PAOX activity in HT22 cells

HT22 cells (mouse hippocampal neuronal cell line) were cultured in Dulbecco's modified Eagle medium, DMEM high glucose supplemented with 10% foetal bovine serum, 4 mM L-glutamine, 100 U/ml penicillin and 100 µg/ml streptomycin (all from Gibco, Thermo Fischer Scientific) and maintained in a 5% CO₂ (v/v) humidified atmosphere at 37 °C. Cells were grown until they reached 70% confluence for a maximum of 25–30 passages.

After trypsinisation, HT22 cell pellets were washed twice with cold PBS, centrifuged (300 × *g* for 5 min), resuspended at a density of about 6 million cells/ml, and incubated in the presence of 2',7'-dichlorodihydrofluorescein diacetate (H₂DCF-DA, Invitrogen) 20 µM, at 37 °C for 20 min in the dark. The cells were then pelleted, washed in PBS, resuspended in PBS containing 5 mM glucose (at about 0.5 million cells/ml) and then incubated in the presence of substrate and/or methoctramine (**10**). All incubations were performed in the dark. Cells in the absence of substrate and compounds were run in parallel and were taken as control samples of the basal H₂O₂ production and DCF fluorescence increments. After 2 min of pre-incubation at 37 °C with methoctramine (**10**), N¹AcSPM 2 µM was added as substrate. DCF fluorescence was monitored at various times for about 30 min (excitation at 488 nm; emission spectra in the range 500–650 nm, peak at about 530 nm). The increase of fluorescence of H₂DCF of each sample was normalised to the protein concentration of the samples, which was determined at the end of each experiment after cell lysis. PAOX activity was calculated as the difference between the specific activity of samples in the presence of substrate and the corresponding control sample (absence of substrate). N¹-Acetylspermine concentration was varied from 1 to 150 µM and, in whole cells, maximum PAOX activity was found at about 5–10 µM; tyramine 1 mM was also used to evaluate the MAO activity in this cellular system. At the end of the experiment, a 200-µM pulse of H₂O₂ was added, to confirm that H₂DCF was not saturated.

After the trypsinisation procedure, HT22 cell lysate was obtained by adding the pelleted cells of 20 mM Hepes (pH 7.5),

1 mM EDTA, and protease inhibitor cocktails (4 million cells/0.1 ml). The lysate was immediately used for amine oxidase activity assays or frozen in liquid nitrogen until use. The amine oxidase activity of lysates was ascertained with the standard Amplex Red horseradish peroxidase assay method reported above, in the presence of various substrates to test the different amine oxidase activity.

Western blot analysis

SDS-polyacrylamide gel electrophoresis was performed according to the standard Laemmli method⁵⁶, with a 10% acrylamide separating gel and a 5% acrylamide spacer gel in Tris-HCl buffer. Samples (HT22 lysates) were solubilised in buffer containing 8 M urea, 2% SDS and 5% β-mercaptoethanol in 62.5 mM Tris-HCl, pH 6.8, boiled at T = 100 °C for about 1 min; 20% glycerol containing bromophenol blue for SDS-PAGE was then added. After electrophoresis, gels were stained for protein determination with Coomassie Brilliant Blue R-250 or for Western blotting. Western blotting was performed overnight at T = 25 °C, on nitrocellulose membranes (at 10 V and 25 mA), with a transfer buffer consisting of 20% methanol, 0.1% SDS in 50 mM Tris and 384 mM Glycine. Non-specific binding sites on membranes were blocked by incubation for 2 h in 3% of bovine serum albumin in TBS (50 mM Tris, 150 mM NaCl, pH = 7.5), prior to incubation with primary antibodies (anti-PAOX 1/400) overnight at 4 °C, washed in TBS with 0.1% Tween 20 for 4–5 h, and then incubated with secondary HRP-conjugated antibodies diluted in blocking solution. Immunoreactive species were detected by chemiluminescence reaction with luminol.

Kinetic and statistical analysis

Steady-state kinetic parameters (V_{max} and K_m) were calculated by fitting the Michaelis-Menten equation to the experimental data (initial rate of reactions vs substrate concentrations) by non-linear regression analysis, with Sigma Plot software, version 9.0 (Jandel Scientific, San Rafael, CA, USA) and the value of the kinetic parameter obtained from the best fit and its SEM are reported.

The mode of inhibition was determined by global fit analysis (GraphPad 5.0 software) of the initial rate of reaction vs substrate concentration curves, in the presence and absence of inhibitor, to fit equations for competitive, mixed, non-competitive and uncompetitive inhibition models. The fit giving the highest r^2 value was selected to calculate the inhibition constant value (K_i).

Unless stated otherwise, the correlation coefficient for linear regression was 0.98 or greater.

For calculating the IC₅₀ value of compound **10** in the cellular system, curve fitting was performed by non-linear regression analysis using the standard “dose-response” curve equation and the Sigma Plot software.

To compare the kinetic parameters of sample with inhibitor with control sample, the Student's *t*-test was applied and $p < .05$ was defined as statistically significant.

All experiments were repeated independently at least three times, and the experimental data were expressed as the mean ± standard deviation (SD).

Results

Selection of polyamine analogues

The aim of this investigation was to discover novel PA derivatives able to discriminate between PAOX and SMOX active sites. Two series of PAs were therefore selected (Table 1). The first series included SPM analogues unsymmetrically substituted on one of the terminal amino groups with different aromatic rings, such as benzene (compound **1**), naphthalene (compound **2**), pyridine (compound **3**) or thiophene (compound **4**). In addition, to evaluate the role of secondary amino groups of SPM on SMOX/PAOX selectivity, PAs **5–8** were included in this study. In particular, the inner nitrogen atoms of compound **4** were replaced with one or two methylene groups (compounds **5** and **6**, respectively) or with oxygen atoms (compound **7**). Compound **8** (Bza-DIADO) is an analogue of compound **1** in which the inner nitrogen atoms were replaced with methylene groups. Compounds **6** and **8** are of particular interest, since they are derivatives of 1,12-diaminododecane (DIADO), a known PAOX inhibitor³³. The second group of compounds includes symmetrically substituted PAs such as *N*1,*N*12-dibenzyl-dodecanediamine (**9**), tetramine methoctramine (**10**) and its derivatives **11–14**. Methoctramine (**10**) is a tetramine bearing a 2-methoxybenzyl moiety on the terminal nitrogen atoms; compounds **11–14** are characterised by inner polymethylene chains of different lengths and features. In particular, compounds **10–14** could give information on the role played by: (i) different lengths of the methylene chain separating the inner nitrogen atoms (**10–12**); (ii) the reduction of the inner flexibility of the molecule, as in compound **13**, which bears a more rigid dipiperidine moiety; (iii) the inner secondary amine functions, by replacing them with amide groups (compound **14**, also known as caproctamine).

Polyamine analogues as potential substrates of SMOX and PAOX

All the compounds listed in Table 1 were first assayed as potential substrates; only some of the unsymmetric, monosubstituted SPM analogues behaved as substrates of SMOX and/or PAOX (see Table 2). Compound **1** has already been reported to be a substrate of SMOX and PAOX (**1** is named BnSPM in Häkkinen et al.⁵⁷).

Table 2 shows that the analogues acting as substrates showed higher affinity (lower K_m values) and specificity for PAOX than for SMOX, as K_m values were in the nanomolar-submicromolar range for PAOX and micromolar range for SMOX. Compounds **2** and **4** were the best substrates, with K_m of 25 and 44 nM for PAOX, and 15 and 10 μ M for SMOX, respectively. In particular, the thiophene derivative of SPM (compound **4**) emerged as the best substrate for SMOX ($K_m=10 \mu$ M with respect to $K_{m\text{SPM}}=490 \mu$ M and catalytic efficiency (V_{\max}/K_m) 19 times that for SPM). For PAOX, the best substrate was compound **2**, bearing the more hydrophobic and hindering naphthalene ring ($K_m=25$ nM with respect to $K_{mN^1\text{AcSPM}}=382$ nM and catalytic efficiency 12 times that of $N^1\text{AcSPM}$). It is worth noting that, among the SPM derivatives (**1–4**), the presence of a less hydrophobic pyridine (**3**) ring reduced the affinity for both enzymes.

These results clearly indicated that the presence of an aromatic ring at one of the terminal amino functions of the SPM chain maintains – and in some cases increases – the substrate profile towards SMOX and PAOX. Conversely, substitution of the two inner nitrogen atoms of the SPM chain with methylene groups (compounds **5**, **6** and **8**) or oxygen atoms (compound **7**), greatly reduces the capability of the enzymes to catalyse the oxidative deamination of these compounds. The poor activity of PAOX for triamine **5** and the lack of activity of SMOX and PAOX towards compounds **6** and **8** support and confirm the crucial role of the inner secondary amine groups of an SPM derivative as a substrate, since their substitution may transform a substrate into an inhibitor.

Screening and selection of potential inhibitors

Compounds which did not behave like SMOX or PAOX substrates, such as **6** and **8**, were tested as potential inhibitors together with compounds **9–14**; chlorhexidine and DIADO were used as reference competitive inhibitors^{33,36}. For the preliminary screening, the effects of a fixed concentration of the compounds (50 μ M) on the kinetic parameters were evaluated. Table 3 lists K_m values and residual V_{\max} relative to the control sample. These data clearly show that all the compounds act mainly by decreasing the affinity of the substrate for both enzymes, with a low or negligible effect on V_{\max} (i.e. the catalytic constant). The more effective

Table 2. Kinetic parameters of compounds 1–8 acting as substrates of murine SMOX and PAOX.

Substrate	SMOX			PAOX		
	K_m (μ M) ($K_{m\text{SPM}}/K_{m\text{PA}}$) ^a	Relative V_{\max}/K_m ^a	Relative V_{\max} ^a	K_m (μ M) ($K_{mN^1\text{AcSPM}}/K_{m\text{PA}}$) ^a	Relative V_{\max}/K_m ^a	Relative V_{\max} ^a
1 ^b	19 ± 3 (26)	9.35	0.32	0.200 ± 0.040 (1.9)	2.5	1.3
2	15 ± 5 (33)	12.9	0.40	0.025 ± 0.004 (15)	12	0.78
3	245 ± 80 (2)	0.414	0.108	0.522 ± 0.043 (0.7)	0.48	0.66
4	10 ± 3 (49)	19	0.31	0.044 ± 0.006 (8.7)	6.52	0.75
5	n.d. ^c	n.a. ^d	n.d. ^c	1.000 ± 0.250 (0.4)	0.27	0.70
6	n.d. ^c	n.a. ^d	n.d. ^c	n.d. ^c	n.a. ^d	n.d. ^c
7	$K_m > 2000$ ^c	0.82	n.d. ^d	n.d. ^c	n.a. ^d	n.d. ^c
8	n.d. ^c	n.a. ^d	n.d. ^c	n.d. ^c	n.a. ^d	n.d. ^c

Enzyme activity was assayed in Hepes 50 mM, pH 7.5, at 37 °C and kinetic analysis as described in the "Materials and methods" section.

^aStandard substrate: SPM for SMOX ($V_{\max}=90 \pm 20$ nM $\text{H}_2\text{O}_2 \text{ min}^{-1}$; $K_{m\text{SPM}} = 495 \pm 130 \mu$ M) and $N^1\text{AcSPM}$ for PAOX ($V_{\max}=107 \pm 12$ nmol $\text{H}_2\text{O}_2 \text{ min}^{-1} \text{ mg}^{-1}$, $K_{mN^1\text{AcSPM}}=382 \pm 160$ nM).

^bCompound **1** is named BnSPM in Häkkinen et al.⁵⁷.

^cNot determinable: saturation not reached in the explored range of compound concentration (maxima concentration tested: 2 mM).

^dNo significant activity at 2 mM of tested compound.

Table 3. Screening of PA analogues as potential inhibitors of SMOX and PAOX.

Compound	SMOX		PAOX	
	K_{mapp} (μ M) (K_{mapp}/K_{m0})	$V_{max\ app}/$ V_{max0}	K_{mapp} (μ M) (K_{mapp}/K_{m0})	$V_{max\ app}/$ V_{max0}
Control	495 \pm 130 (1)	1	0.38 \pm 0.16 (1)	1
5	1060 \pm 70 (2.1)	0.77	Substrate	Substrate
6	1740 \pm 140 (1.84)	0.82	89 \pm 12 (234)	0.99
7	Poor substrate	Poor substrate	60 \pm 16 (157)	1.2
8	1990 \pm 230 (2.1)	0.69	25 \pm 2 (66)	0.88
9	1135 \pm 141 (2.3)	1.01	41 \pm 221 (108)	1.0
10	8940 \pm 1600 (18)	0.67	n.d. ^a	n.d. ^a
11	7770 \pm 580 (15.7)	0.71	n.d. ^a	n.d. ^a
12	5820 \pm 630 (11.7)	0.62	n.d. ^a	n.d. ^a
13	2501 \pm 490 (5.0)	0.69	134 \pm 32 (350)	0.80
14	598 \pm 156 (1.21)	0.53	43 \pm 9 (112)	1.05
DIADO	600 \pm 100 (1.2)	0.9	3.40 \pm 0.26 (9)	1.3
Chlorhexidine ^b	1402 \pm 124 (2.8)	0.9	1.90 \pm 0.12 (5)	1.2

Kinetic parameters were determined in the presence of 50 μ M of the PA, with the exception of Chlorhexidine, in standard assay condition as described in the "Materials and methods" section.

^aNot determinable: saturation not reached in the explored range of substrate concentration (maxima [N^1 AcSPM] = 0.6 mM).

^b[Chlorhexidine] = 5 μ M.

compounds were methoctramine and its derivatives (compounds **10–12**), in particular towards PAOX: the affinity for the substrate decreased more than ten times in the case of SMOX and much more in the case of PAOX (not determinable at this inhibitor concentration). Compound **13**, bearing a rigid dipiperidine moiety, and compound **14**, containing the inner amide functions, were very effective in decreasing the affinity of substrate for PAOX (K_m increase of more than two orders of magnitude), but not for SMOX. The unsymmetrically substituted SPM analogues appeared in general less effective than methoctramine derivatives, in particular towards SMOX. Compounds **6**, **8** and **9**, representing derivatives of DIADO (PAOX competitive inhibitor), reduced the PAOX affinity for the substrate by about one order of magnitude, being more effective as inhibitors than their precursor DIADO. On this basis, compounds **10–13**, the most potent in decreasing the affinity of the substrate for SMOX and PAOX, were selected for kinetic characterisation.

Kinetic characterisation of the most effective inhibitors of SMOX and PAOX activity

To investigate the type of inhibition of the selected compounds, the kinetic parameters (V_{max} , K_m and V_{max}/K_m) of SMOX and PAOX were determined in the presence of various concentrations of these PA analogues, with SPM and N^1 AcSPM as substrates, respectively. All the tested compounds were found to act as competitive inhibitors, as clearly shown in Figure 1. The Lineweaver-Burk plots (double reciprocal plots) of the initial rate of reaction in the presence of various concentrations of methoctramine derivatives (**10–13**) did in fact show that only the K_m values (intercept on the x-axis represents $-1/K_m$) change in the presence of the

compounds. Table 4 lists the inhibition constant (K_i) and selectivity (K_{iSMOX}/K_{iPAOX}) values. These results clearly show that methoctramine and its derivatives (**10–13**) mainly target PAOX, and, in particular, methoctramine (**10**), with a K_i of 10 nM for PAOX vs 1200 nM for SMOX (selectivity 1:120), resulted the most potent and selective inhibitor. The decrease in the length of the inner polymethylene chain, as in **11** and **12**, led to a reduced inhibitory potency and selectivity ($K_{iSMOX}: K_{iPAOX}$ 9:1 for **12**). A sterically constrained dipiperidine chain, as in **13** with respect to **10**, also strongly affected inhibitory potency and specificity ($K_i=10$ nM of **10** vs $K_i=440$ nM of **13** for PAOX). In addition, all these methoctramine derivatives were found to be more potent PAOX inhibitors than the reference inhibitors (chlorhexidine and DIADO). In the case of SMOX, compounds **10–13** showed increased potency with respect to DIADO and similar potency with respect to chlorhexidine.

Docking simulations of selected compounds on PAOX crystal structure

The structural bases of the binding of selected substrates and inhibitors to PAOX and SMOX were analysed by docking simulations via AutoDock Vina (see Materials and Methods for details). Figure 2 shows the PAOX complexes obtained by docking simulations with substrates **2** and **4**. In both cases, the compounds bind to the PAOX active site with a conformation very similar to that observed in the PAOX crystal structure for substrate N^1 AcSPM, the terminal primary amino group of the compound being located near Phe201 and the hydrophobic moiety on the other end of the molecule contacting Phe375. Both compounds are characterised by the presence of secondary amino groups and this is a

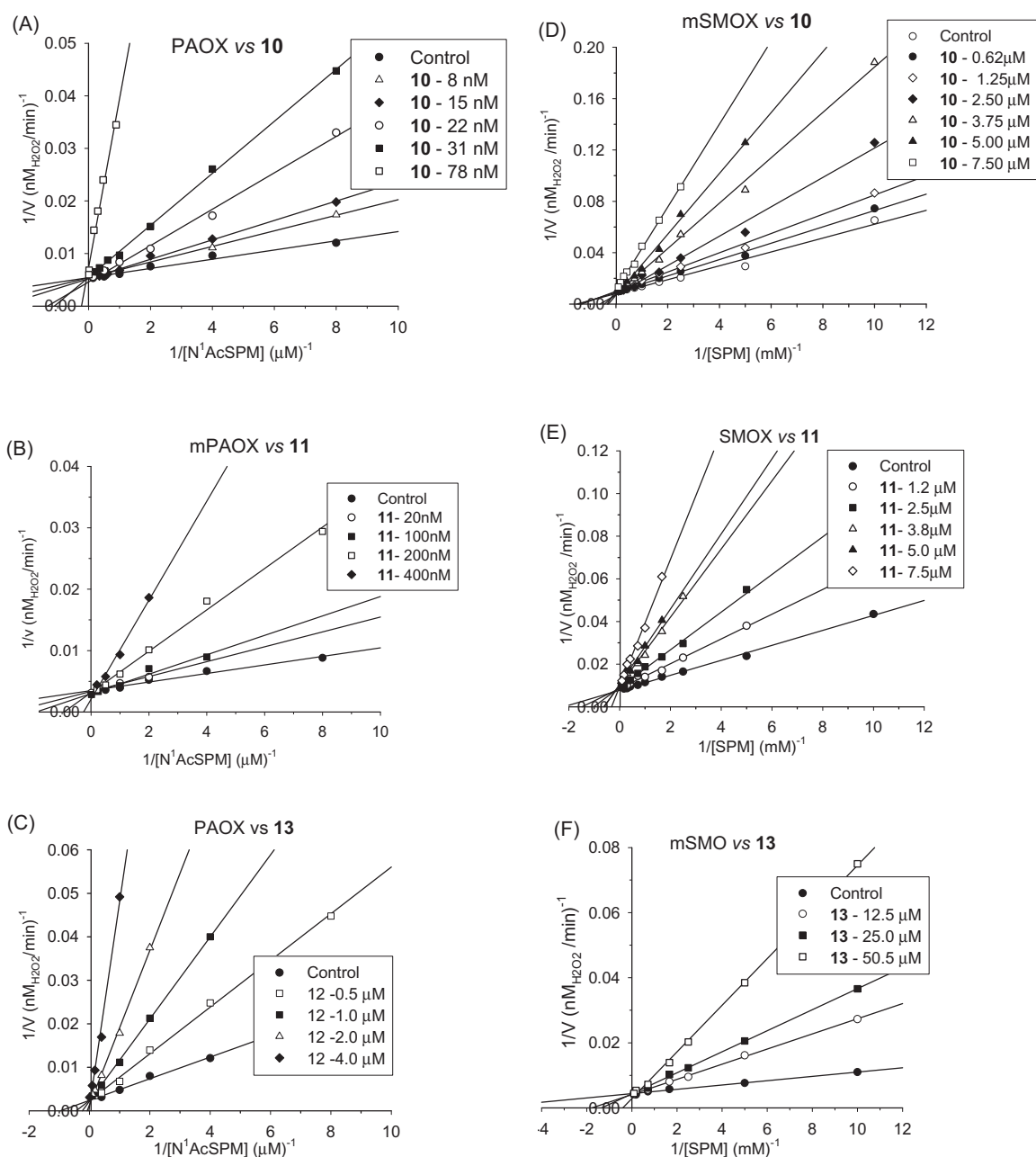


Figure 1. Compounds **10**, **11** and **13** act as competitive inhibitors of murine PAOX and SMOX. Double reciprocal plots of PAOX activity in the presence of various concentration of compound **10** (A), **11** (B) and **13** (C); Double reciprocal plots of SMOX activity in the presence of various concentration of compound **10** (D), compound **11** (E) and **13** (F). Continuous lines are the results of linear regression analysis of experimental data ($r > 0.98$). The K_i values for the competitive mode of inhibition were calculated by global fit analysis (GraphPad 5.0 software) and are reported in Table 4.

prerequisite for a PA to act as a substrate of animal polyamine oxidases, which, in fact, oxidise the carbon atom in *eso* with respect to a secondary amino group. Thus, the binding mode observed and the vicinity of the carbon atom in *eso* of the compounds to the redox-active N5 atom of FAD (as observed for the experimental structure of the PAOX- N^1 AcSPM complex), explain fairly well their ability to act as substrates.

Inhibitors **10–13** are all predicted to bind in the PAOX active site, matching the competitive nature of their inhibition. Analysis of the docking complexes (Figure 3) shows that all the inhibitors mainly bind through hydrophobic interactions with Trp62 and Phe375. However, in the case of **10**, a hydrogen bond was

Table 4. Inhibition constant values of the most potent methotramine derivatives and comparison with the reference inhibitors, chlorhexidine and DIADO.

Inhibitor	SMOX K_i (μ M)	PAOX K_i (nM)	Selectivity $K_{iSMOX} : K_{iPAOX}$
10	1.2 ± 0.1	10.0 ± 1.5	120:1
11	1.9 ± 0.2	47 ± 5	40:1
12	4.6 ± 0.2	525 ± 84	9:1
13	7.5 ± 2.7	439 ± 84	17:1
Chlorhexidine	3.8 ± 0.2	$1.25 \pm 0.6 \times 10^3$	3:1
DIADO	$>10^3$ ^a	$6.3 \pm 0.8 \times 10^3$	$>150:1$

Kinetic experiments and analysis as described in the "Materials and methods" section.

^afrom Bianchi et al.³³

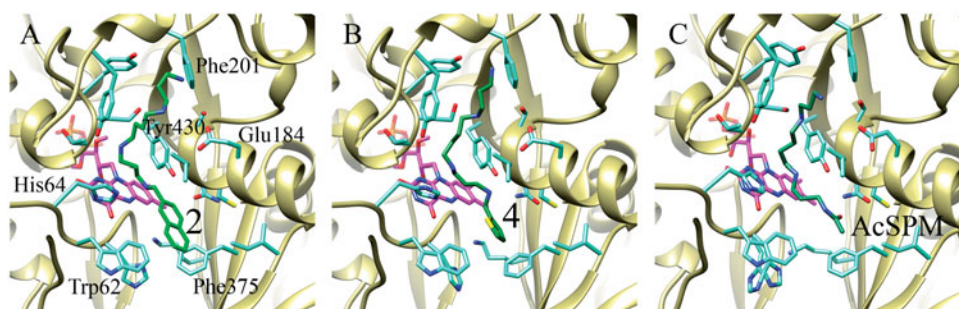


Figure 2. Best docking poses obtained for the substrates 2 (A) and 4 (B) compared with the experimentally determined structure of the PAOX-N¹AcSPM complex (C).

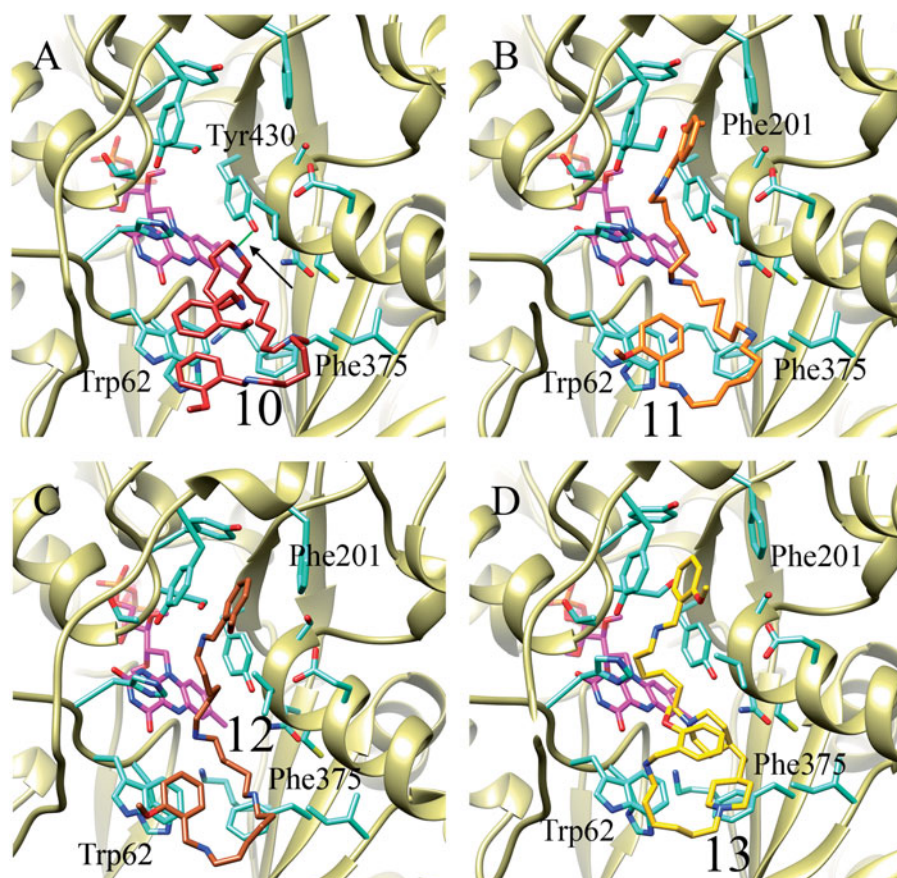


Figure 3. Best docking poses obtained for the inhibitors structurally related to methoctramine (10–13) in complex with PAOX. Compound 10 in panel A, 11 in B, 12 in C and 13 in D. Hydrogen bond between Tyr430 and the inhibitor 10 is highlighted in green and indicated by a black arrow.

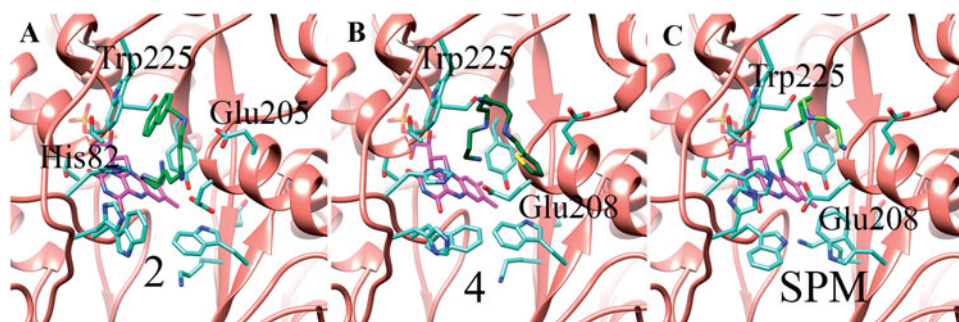


Figure 4. Representative docking poses obtained for the substrates 2 (A), 4 (B) and SPM (C) onto the SMOX structural model. In each case the representative pose shown in the figure is one of the nine top-scoring poses according to Autodock Vina scoring function.

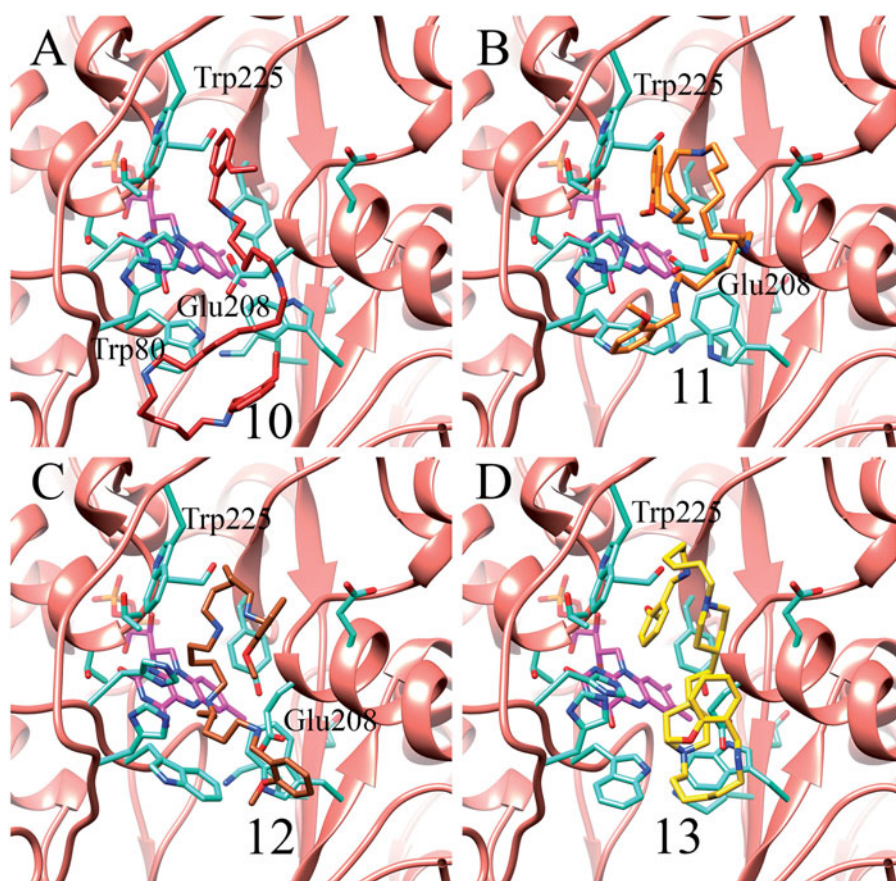


Figure 5. Representative docking poses obtained for the inhibitors 10–13 in complex with the SMOX structural model. Compound 10 in panel A, 11 in B, 12 in C and 13 in D. In each case the representative pose shown in the figure is one of the nine top-scoring poses according to Autodock Vina scoring function.

observed between one of the inhibitor's amino groups and Tyr430. In addition, the latter inhibitor adopts a "folded" conformation within the PAOX active site, probably due to its length, as the 2-methoxybenzyl rings stack on to each other on Trp62. This intramolecular interaction and the hydrogen bond formed with Tyr430 may lie at the root of the high affinity for PAOX measured for this inhibitor.

For completeness, docking simulations of substrates and inhibitors were also carried out on a recently published SMOX molecular model based on the PAOX crystal structure³⁹. Figure 4 shows the SMOX complexes obtained by docking simulations with substrates 2, 4 and SPM. Both the synthetic substrates and the natural substrate are predicted to bind through hydrophobic interactions with Trp225. Additional electrostatic interactions with His82 and Glu205 are predicted to stabilise compound 2. Similarly, both 4 and SPM are predicted to interact with Glu208. It is worth noting that, in SMOX, the primary amino group points towards the FAD cofactor, unlike PAOX. Also in the case of SMOX, inhibitors 10–13 are all predicted to bind in the active site, once again matching the competitive nature of their inhibition. Analysis of the docking complexes (Figure 5) indicates that all the inhibitors mainly act through hydrophobic interaction with Trp225. An additional hydrophobic interaction with Trp80 was observed in the case of the compound 10 complex, the most potent according to the kinetic results. Lastly, in the case of compounds 10–12-SMOX complexes, electrostatic interactions were also observed between the inhibitors' secondary amine groups and Glu208.

Biological activity of methoctramine as inhibitor: selectivity towards other AOs and in cell activity

In order to evaluate the potential effects of the PA analogues on a cellular system and then in a more complex biological system, it is important to collect information on their selectivity also on other types of amine oxidases. In Table 5, the behaviour and the kinetic parameters of compounds 2, 4 (the best SMOX and PAOX substrates), 10 and 13 (the best inhibitors) were compared with those previously obtained with human semicarbazide-sensitive amine oxidase/vascular adhesion protein-1 (SSAO/VAP-1)⁴⁶ and MAOs (human MAO A and MAO B)⁴⁷. It clearly appears that compound 10 emerged as the best and most selective PAOX inhibitor. The less potent and selective compound 13 ($K_{iSMOX}/K_{iPAOX} = 17/1$) was previously found to be a very poor, almost unaffected inhibitor of MAOs and SSAO/VAP-1 ($K_i > 100 \mu\text{M}$) in comparison with PAOX and SMOX. It is to emphasise that the selectivity profile of methoctramine versus the other amine oxidases is much better in comparison with that of DIADO, which is a selective murine PAOX inhibitor, ($K_i = 8 \mu\text{M}$ for PAOX vs $K_i = 1 \text{mM}$ for SMOX)³³, but also an excellent substrate of the human SSAO/VAP-1 ($K_m = 13 \mu\text{M}$) and of MAO A⁵⁸, differently from methoctramine.

In addition, Table 5 shows that compound 2, the best PAOX substrate, is not active on MAOs and SSAO/VAP-1, whereas compound 4, the best SMOX substrate, was found to act as a competitive inhibitor of MAO B.

On these bases, we focussed attention on the most selective compound 10 and evaluated its inhibitory activity in the

Table 5. Inhibition constant (K_i) or K_m values of the most effective inhibitors (**10** and **13**) or substrates (**2** and **4**) of SMOX and PAOX in comparison with the K_i or K_m values for human MAO A, MAO B and SSAO/VAP-1.

Compound	MAO A	MAO B	SSAO/VAP-1	SMOX	PAOX
2	n.a. ^{a,b}	n.a. ^{a,b}	n.a. ^{a,b}	$K_{m,2} = 15 \mu\text{M}$ Substrate	$K_{m,2} = 25 \text{ nM}$ Substrate
4	$K_i = 226 \mu\text{M}$ ^b	$K_i = 23 \mu\text{M}$ ^b	n.e. ^{a,b}	$K_{m,4} = 10 \mu\text{M}$ Substrate	$K_{m,4} = 44 \text{ nM}$ Substrate
10	n.a. ^a	n.a. ^{a,c}	n.a. ^{a,c}	$K_i = 1.2 \mu\text{M}$	$K_i = 10 \text{ nM}$
13	$K_i > 100 \mu\text{M}$	$K_i = 323 \mu\text{M}$ ^c	$K_i = 111 \mu\text{M}$ ^c	$K_i = 7.5 \mu\text{M}$	$K_i = 439 \text{ nM}$

^an.a. not active as substrate or inhibitor up to 50 μM concentration.

^bfrom Bonaiuto et al. 2013⁴⁷.

^cfrom Bonaiuto et al. 2012⁴⁶.

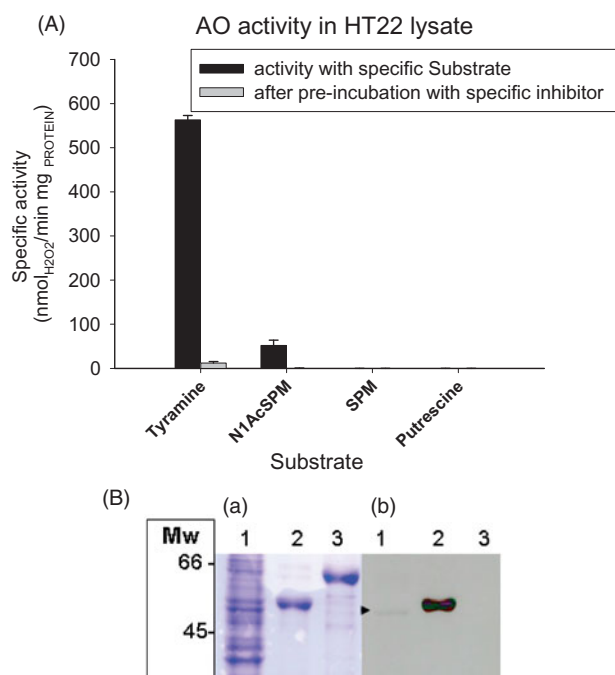


Figure 6. Amine oxidase activity and immunodetection of PAOX protein in HT22 cell lysate. (A) Amine oxidase activity was carried out in HEPES buffer, using the Amplex Red-horseradish peroxidase assay method, at 37 °C and specific substrates for the different type of amine oxidases: tyramine (1mM) for MAOs; N1AcSPM (0.25 mM) for APAOX; SPM (10mM) for SMOX and Putrescine (10mM) for diamine oxidases. Activity with tyramine was decreased to 2% with respect to control sample, after pre-incubation of sample with pargyline (specific MAO inhibitor); activity with N1AcSPM was no detectable after pre-incubation of sample with MDL 72572. The data were presented as the means \pm SD. Statistical significance: p -values $< .05$ when control (no inhibitor) compared with sample pre-incubated with inhibitor (paired Student's t -test). (B) Immunodetection of PAOX protein in HT22 cells lysate. (a): SDS-PAGE 10%; (b) nitrocellulose membranes immunostained with anti-PAOX. Lane 1: lysate from HT22 cells (20 μg); Lane 2: purified mouse PAOX (1 μg); in Lane 3: purified mouse SMOX (1 μg).

mouse hippocampal HT22 cell line. This cell line was chosen because, with N¹AcSPM as substrate, significant PAOX activity has been found in its cell lysate. In addition, methoctramine (**10**) has already been evaluated on HT22 cells (at micromolar concentrations) as an M2/M4 muscarinic receptor antagonist⁵⁹, proving that this cell line, widely used to evaluate neuroprotective agents^{60–62}, possesses the property of correcting cholinergic neuron hypofunctionality by increasing the release of acetylcholine.

The presence of other amine oxidases in HT22 cell lysates was evaluated with specific substrates: tyramine for MAO, SPM for SMOX, and putrescine for diamine oxidase. The results (Figure 6(A)) confirmed the known presence of MAOs (as previously reported⁶¹) and the absence of SMOX and diamine oxidase

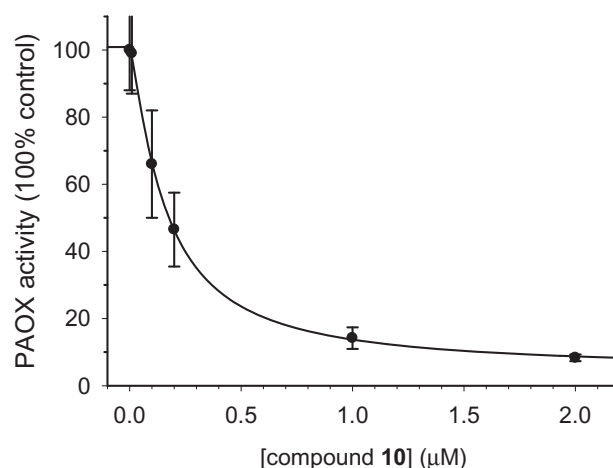


Figure 7. Effect of compound **10** on PAOX activity in HT22 cells. PAOX activity in HT22 cells was determined by using H₂DCF-DA as fluorescence probe for the detection of the hydrogen peroxide generation. Cells loaded with H₂DCF-DA were pre-incubated with **10** before the addition of substrate (N¹AcSPM), as describe in the "Experimental procedure" Polyamine oxidase activity was calculated as the difference between the change in fluorescence of samples in the presence of substrate and the corresponding control sample (absence of substrate). Results were normalised to protein content of cells. Continuous line is the result of the best fitting of the "dose-response" curve to experimental data using the SigmaPlot 9.0 software ($IC_{50} = 160 \pm 10 \text{ nM}$; $r > 0.98$; $p < .05$).

activity. In addition, activity on N¹AcSPM was found to be inhibited by pre-incubation with the irreversible inhibitor MDL 72527, supporting the presence of PAOX. The expression of PAOX was also demonstrated by immunodetection of the protein in HT22 lysates (Figure 6(B)). On this basis, the PAOX activity was evaluated on whole HT22 cells, with N¹AcSPM as substrate, in both the presence and absence of **10**. The results (Figure 7) confirm the effectiveness of **10** in inhibiting PAOX activity in this cellular model, with an $IC_{50} = 160 \pm 10 \text{ nM}$, about 16 times higher than the K_i value found with the recombinant enzyme *in vitro*.

Discussion

With the aim to develop novel anticancer agents and therapeutic approaches, many researches have been focussed on the design of PA analogues to target the catabolic PA pathway^{1,14,16,18}. In particular, the discovery of PA analogues acting as substrates or inhibitors of PAOX and SMOX deserves great interest in the search of anticancer and chemopreventive agents.

According to the literature, a novel anticancer pharmacological approach proposes the use of PA analogues as substrates of poly-amino oxidases, to induce cell death. It has been demonstrated that, after bovine serum amino oxidase delivering into B16 melanoma cells, a slow release of endogenous SPM metabolites (H₂O₂ and acrolein) was induced, leading to apoptosis and inhibition of

tumour growth^{12,13,63,64}. In previous studies, among the various types of PA analogues investigated to discover selective SMOX vs PAOX substrates^{24,57,65–67}, the pentamine *N*¹-(3-aminopropyl)-*N*⁴-(3-((3-aminopropyl)amino)propyl)butane-1,4-diamine pentahydrochloride (3343 in Takao et al.⁶⁷) emerged as a very good substrate of SMOX (V_{max}/K_m about 2 order of magnitude higher than that for SPM and no data on PAOX available).

On this basis, in the present study, unsymmetrically and symmetrically substituted polyamines structurally related to SPM (compounds **1–9**) and methoctramine (compounds **10–14**) were evaluated by a kinetic approach as potential substrates or inhibitors of SMOX and PAOX enzymes. Among the unsymmetrical SPM derivatives, we found that the presence of the naphthalene and thiophene ring at one terminal end (compounds **2** and **4**, respectively) confers a strong affinity and very high catalytic efficiency for PAOX and SMOX, respectively, much higher than those of their physiological substrates, *N*¹AcSPM and SPM.

According to the new pharmacological approach described above, exploiting the amino oxidase activity on PA substrates, compound **2**, which joins both high catalytic efficiency and selectivity in comparison with other amine oxidases (Table 5), could be considered a valuable starting point for developing new anti-cancer agents. The novel substrates (PA analogues, free or after conjugation with nanoparticles) could be delivered into cancer cells highly expressing SMOX and/or PAOX to generate *in situ* cytotoxic products. In addition, the low K_m and high V_{max}/K_m values of substrates, such as compounds **2** and **4**, could allow their use in clinical application at low concentration, reducing drastically side effects^{12,13}.

Interestingly, several studies have highlighted the relevant role of PAOX and SMOX in carcinogenesis, and the level of these enzymes has been or high^{29,68,69} in some types of cancers. The aberrant activation of PA-driven oxidative stress due to high level of SMOX and leading to tumorigenesis, supports a different and emerging pharmacological approach concerning the development of PA analogues capable to selectively inhibit SMOX or PAOX. These inhibitors could be valuable probes to investigate the carcinogenesis pathway and could have potential as chemopreventive agents^{18,20}.

In this study, we found that unlike unsymmetrical SPM analogues, the symmetrically substituted methoctramine analogues behaved mainly as PAOX inhibitors.

The main finding emerging from our analyses is that compound **10** (methoctramine), already known as a selective M2/M4 muscarinic receptor antagonist⁷⁰, acts also as a potent reversible murine PAOX inhibitor ($K_i=10$ nM on the recombinant enzyme), with excellent selectivity with respect to SMOX and other amine oxidases (MAOs and SSAO/VAP-1). To our knowledge, this is the most potent competitive inhibitor of PAOX found so far. Preliminary biological data support its effectiveness at submicromolar concentration in inhibiting PAOX activity in HT22 cells.

Taking into account the low cytotoxicity of compound **10** (methoctramine)^{71,72} and that, at a concentration of 10 μ M, it did not significantly affect other targets of PA metabolism (such as ODC and SSAT)⁷¹, methoctramine emerged as a very promising tool in the design of potential drugs targeting the PA catabolism pathway.

The availability of selective inhibitors of PAOX could enable to discriminate between the role played by SMOX compared to PAOX in the inflammation-induced carcinogenesis and in other pathologies, in view of new therapeutic applications.

Further studies are necessary and are in progress to evaluate the novel SMOX and PAOX substrates (compounds **2** and **4**) in

cancer cells and to deeply investigate the inhibitory behaviour of methoctramine in different cellular systems and in systems expressing both SMOX and PAOX.

Acknowledgements

The authors thank the “International Polyamine Foundation - ONLUS” for the availability to look up in the Polyamine documentation. Dr. Andrea Pasquadibisceglie is gratefully acknowledged for his contribution to docking studies.










Disclosure statement

No potential conflict of interest was reported by the authors.

Funding

This research was supported by institutional grants from the University of Padova, Italy (Fondi di ricerca di Ateneo, Ex 60% 2015, code 60A06-1707/15) to M.L.D.P. and from the University of Bologna, Italy (RFO 2015–2016) to A.M. (Anna Minarini).

ORCID

Maria Luisa Di Paolo  <http://orcid.org/0000-0002-2370-9333>
 Manuela Cervelli  <http://orcid.org/0000-0001-8535-8279>
 Paolo Mariottini  <http://orcid.org/0000-0003-1044-7108>
 Alessia Leonetti  <http://orcid.org/0000-0002-7445-8415>
 Fabio Polticelli  <http://orcid.org/0000-0002-7657-2019>
 Michela Rosini  <http://orcid.org/0000-0003-3750-2728>
 Andrea Milelli  <http://orcid.org/0000-0003-2285-7403>
 Enzo Agostinelli  <http://orcid.org/0000-0002-2508-8868>
 Anna Minarini  <http://orcid.org/0000-0002-4905-0944>

References

1. Nowotarski SL, Woster PM, Casero RA. Jr., Polyamines and cancer: implications for chemotherapy and chemoprevention. *Expert Rev Mol Med* 2013;15:e3.
2. Cervelli M, Angelucci E, Germani F, et al. Inflammation, carcinogenesis and neurodegeneration studies in transgenic animal models for polyamine research. *Amino Acids* 2014; 46:521–30.
3. Gerner EW, Meyskens FL. Jr., Polyamines and cancer: old molecules, new understanding. *Nat Rev Cancer* 2004;4: 781–92.
4. Seiler N. Oxidation of polyamines and brain injury. *Neurochem Res* 2000; 25:471–90.
5. Tomitori H, Usui T, Saeki N, et al. Polyamine oxidase and acrolein as novel biochemical markers for diagnosis of cerebral stroke. *Stroke* 2005;36:2609–13.
6. Park MH, Igarashi K. Polyamines and their metabolites as diagnostic markers of human diseases. *Biomol Ther (Seoul)* 2013;21:1–9.
7. Pegg AE. Toxicity of polyamines and their metabolic products. *Chem Res Toxicol* 2013;26:1782–800.
8. Cervelli M, Amendola R, Polticelli F, Mariottini P. Spermine oxidase: ten years after. *Amino Acids* 2012;42:441–50.
9. Cervelli M, Bellavia G, D’Amelio M. A new transgenic mouse model for studying the neurotoxicity of spermine oxidase

- dosage in the response to excitotoxic injury. *PLoS One* 2013;8:e64810.
10. Cervetto C, Vergani L, Passalacqua M, et al. Astrocyte-dependent vulnerability to excitotoxicity in spermine oxidase-overexpressing mouse. *Neuromolecular Med* 2016;18:50–68.
 11. Sharmin S, Sakata K, Kashiwagi K, et al. Polyamine cytotoxicity in the presence of bovine serum amine oxidase. *Biochem Biophys Res Commun* 2001;282:228–35.
 12. Agostinelli E, Belli F, Molinari A, et al. Toxicity of enzymatic oxidation products of spermine to human melanoma cells (M14): sensitization by heat and MDL 72527. *Biochim Biophys Acta* 2006;1763:1040–50.
 13. Agostinelli E, Condello M, Tempera G, et al. The combined treatment with chloroquine and the enzymatic oxidation products of spermine overcomes multidrug resistance of melanoma M14 ADR2 cells: a new therapeutic approach. *Int J Oncol* 2014;45:1109–22.
 14. Wallace HM, Fraser AV. Inhibitors of polyamine metabolism: review article. *Amino Acids* 2004;26:353–65.
 15. Amendola R, Cervelli M, Tempera G, et al. Spermine metabolism and radiation-derived reactive oxygen species for future therapeutic implications in cancer: an additive or adaptive response. *Amino Acids* 2014;46:487–98.
 16. Casero RA, Jr, Marton LJ. Targeting polyamine metabolism and function in cancer and other hyperproliferative diseases. *Nat Rev Drug Discov* 2007;6:373–90.
 17. Calcabrini A, Arancia G, Marra M, et al. Enzymatic oxidation products of spermine induce greater cytotoxic effects on human multidrug-resistant colon carcinoma cells (LoVo) than on their wild-type counterparts. *Int J Cancer* 2002;99:43–52.
 18. Murray-Stewart TR, Woster PM, Casero RA. Jr., Targeting polyamine metabolism for cancer therapy and prevention. *Biochem J* 2016;473:2937–53.
 19. Casero RA, Jr, Pegg AE. Polyamine catabolism and disease. *Biochem J* 2009;421:323–38.
 20. Murray Stewart T, Dunston TT, Woster PM, Casero RA. Jr., Polyamine catabolism and oxidative damage. *J Biol Chem* 2018;293:18736–45.
 21. Pozzi MH, Gawandi V, Fitzpatrick PF. Mechanistic studies of para-substituted N,N'-dibenzyl-1,4-diaminobutanes as substrates for a mammalian polyamine oxidase. *Biochemistry* 2009;48:12305–13.
 22. Cervelli M, Salvi D, Polticelli F, et al. Structure-function relationships in the evolutionary framework of spermine oxidase. *J Mol Evol* 2013;76:365–70.
 23. Polticelli F, Salvi D, Mariottini P, et al. Molecular evolution of the polyamine oxidase gene family in Metazoa. *BMC Evol Biol* 2012;12:90.
 24. Wang Y, Hacker A, Murray-Stewart T, et al. Properties of recombinant human N1-acetyl polyamine oxidase (hPAO): potential role in determining drug sensitivity. *Cancer Chemother Pharmacol* 2005;56:83–90.
 25. Cervelli M, Bellini A, Bianchi M, et al. Mouse spermine oxidase gene splice variants. Nuclear subcellular localization of a novel active isoform. *Eur J Biochem* 2004;271:760–70.
 26. Cervelli M, Fratini E, Amendola R, et al. Increased spermine oxidase (SMO) activity as a novel differentiation marker of myogenic C2C12 cells. *Int J Biochem Cell Biol* 2009;41:934–44.
 27. Bongers KS, Fox DK, Kunkel SD, et al. Spermine oxidase maintains basal skeletal muscle gene expression and fiber size and is strongly repressed by conditions that cause skeletal muscle atrophy. *Am J Physiol Endocrinol Metab* 2015;308:E144–58.
 28. Bonaiuto E, Grancara S, Martinis P, et al. A novel enzyme with spermine oxidase properties in bovine liver mitochondria: identification and kinetic characterization. *Free Radic Biol Med* 2015;82:88–99.
 29. Goodwin AC, Jadallah S, Toubaji A, et al. Increased spermine oxidase expression in human prostate cancer and prostatic intraepithelial neoplasia tissues. *Prostate* 2008;68:766–72.
 30. Chaturvedi R, Asim M, Romero-Gallo J, et al. Spermine oxidase mediates the gastric cancer risk associated with *Helicobacter pylori* CagA. *Gastroenterology* 2011;141:1696–708.
 31. Hu T, Sun D, Zhang J, et al. Spermine oxidase is upregulated and promotes tumor growth in hepatocellular carcinoma. *Hepatol Res* 2018;48:967–77.
 32. Murray-Stewart T, Sierra JC, Piazzuelo MB, et al. Epigenetic silencing of miR-124 prevents spermine oxidase regulation: implications for *Helicobacter pylori*-induced gastric cancer. *Oncogene* 2016;35:5480–8.
 33. Bianchi M, Polticelli F, Ascenzi P, et al. Inhibition of polyamine and spermine oxidases by polyamine analogues. *FEBS J* 2006;273:1115–23.
 34. Bey P, Bolkenius FN, Seiler N, Casara PN. 2,3-Butadienyl-1,4-butanediamine derivatives: potent irreversible inactivators of mammalian polyamine oxidase. *J Med Chem* 1985;28:1–2.
 35. Moriya SS, Miura T, Takao K, et al. Development of irreversible inactivators of spermine oxidase and N¹-acetyl polyamine oxidase. *Biol Pharm Bull* 2014;37:475–80.
 36. Cervelli M, Polticelli F, Fiorucci L, et al. Inhibition of acetyl polyamine and spermine oxidases by the polyamine analogue chlorhexidine. *J Enzyme Inhib Med Chem* 2013;28:463–7.
 37. Sjögren T, Wassvik CM, Snijder A, et al. The structure of murine N¹ acetylspermine oxidase reveals molecular details of vertebrate polyamine catabolism. *Biochemistry* 2017;56:458–67.
 38. Tavladoraki P, Cervelli M, Antonangeli F, et al. Probing mammalian spermine oxidase enzyme-substrate complex through molecular modeling, site-directed mutagenesis and biochemical characterization. *Amino Acids* 2011;40:1115–26.
 39. Leonetti A, Cervoni L, Polticelli F, et al. Spectroscopic and calorimetric characterization of spermine oxidase and its association forms. *Biochem J* 2017;474:4253–68.
 40. Cervelli M, Angelucci E, Stano P, et al. The Glu²¹⁶/Ser²¹⁸ pocket is a major determinant of spermine oxidase substrate specificity. *Biochem J* 2014; 461:453–9.
 41. Polticelli F, Basran J, Faso C, et al. Lys300 plays a major role in the catalytic mechanism of maize polyamine oxidase. *Biochemistry* 2005;44:16108–20.
 42. Henderson Pozzi M, Gawandi V, Fitzpatrick PF. pH dependence of a mammalian polyamine oxidase: insights into substrate specificity and the role of lysine 315. *Biochemistry* 2009;48:1508–16.
 43. Minarini A, Milelli A, Tumiatti V, et al. Synthetic polyamines: an overview of their multiple biological activities. *Amino Acids* 2010;38:383–92.
 44. Melchiorre C, Bolognesi ML, Minarini A, et al. Polyamines in drugs discovery: from the universal template approach to the multitarget-directed ligand design strategy. *J Med Chem* 2010;53:5906–14.

45. Bradford MM. A rapid and sensitive method for the quantitation of microgram quantities of protein utilizing the principle of protein-dye binding. *Anal Biochem* 1976;72:248–54.
46. Bonaiuto E, Minarini A, Tumiatti V, et al. Synthetic polyamines as potential amine oxidase inhibitors: a preliminary study. *Amino Acids* 2012;42:913–28.
47. Bonaiuto E, Milelli A, Cozza G, et al. Novel polyamine analogues: from substrates towards potential inhibitors of monoamine oxidases. *Eur J Med Chem* 2013;70:88–101.
48. Melchiorre C, Minarini A, Quaglia W, Tumiatti V. Methocramine. *Drugs Future* 1989;14:628–31.
49. Minarini A, Budriesi R, Chiarini A, et al. Further investigation on methocramine-related tetraamines: effects of terminal N-substitution and of chain length separating the four nitrogens on M₂ muscarinic receptor blocking activity. *Farmacol* 1991;46:1167–78.
50. Tumiatti V, Minarini A, Milelli A, et al. Structure-activity relationships of methocramine-related polyamines as muscarinic antagonist: effect of replacing the inner polymethylene chain with cyclic moieties. *Bioorg Med Chem* 2007;15:2312–21.
51. Melchiorre C, Andrisano M, Bolognesi ML, et al. Acetylcholinesterase noncovalent inhibitors based on a polyamine backbone for potential use against Alzheimer's disease. *J Med Chem* 1998;41:4186–9.
52. Zhou N, Panchuk-Voloshina N. A one-step fluorometric method for the continuous measurement of monoamine oxidase activity. *Anal. Biochem* 1997;253:169–74.
53. Corazza A, Stevanato R, Di Paolo ML, et al. Effect of phosphate ion on the activity of bovine plasma amine oxidase. *Biochem Biophys Res Commun* 1992;189:722–7.
54. Ionescu CM, Sehnal D, Falginella FL, et al. AtomicChargeCalculator: interactive web-based calculation of atomic charges in large biomolecular complexes and drug like molecules. *J Cheminform* 2015;7:50.
55. Trott O, Olson AJ. AutoDock Vina: improving the speed and accuracy of docking with a new scoring function, efficient optimization, and multithreading. *J Comp Chem* 2010;31:455–61.
56. Laemmli UK. Cleavage of structural proteins during the assembly of the head of bacteriophage T4. *Nature* 1970;227:680–5.
57. Häkkinen MR, Hyvönen M, Auriola S, et al. Metabolism of N-alkylated spermine analogues by polyamine and spermine oxidases. *Amino Acids* 2010;38:369–81.
58. Bonaiuto E, Lunelli M, Scarpa M, et al. A structure-activity study to identify novel and efficient substrates of the human semicarbazide-sensitive amine oxidase/VAP-1 enzyme. *Biochimie* 2010;92:858–68.
59. Liu J, Li L, Suo WZ. HT22 hippocampal neuronal cell line possesses functional cholinergic properties. *Life Sci* 2009;84:267–71.
60. Lee DS, Ko W, Kim DC, et al. Cudarflavone B provides neuroprotection against glutamate-induced mouse hippocampal HT22 cell damage through the Nrf2 and PI3K/Akt signaling pathways. *Molecules* 2014;19:10818–31.
61. Cao X, Wei Z, Gabriel GG, et al. Calcium-sensitive regulation of monoamine oxidase-A contributes to the production of peroxyradicals in hippocampal cultures: implications for Alzheimer disease-related pathology. *BMC Neurosci* 2007;8:73.
62. Sawa K, Uematsu T, Korenaga Y, et al. Krebs cycle intermediates protective against oxidative stress by modulating the level of reactive oxygen species in neuronal HT22. *Cells* 2017; 6:E21.
63. Averill-Bates DA, Cherif A, Agostinelli E, et al. Anti-tumoral effect of native and immobilized bovine serum amine oxidase in a mouse melanoma model. *Biochem Pharmacol* 2005;69:1693–704.
64. Averill-Bates DA, Ke Q, Tanel A, et al. Mechanism of cell death induced by spermine and amine oxidase in mouse melanoma cells. *Int J Oncol* 2008;32:79–88.
65. Weisell J, Hyvönen MT, Häkkinen MR, et al. Synthesis and biological characterization of novel charge-deficient spermine analogues. *J Med Chem* 2010;53:5738–48.
66. Ucal S, Häkkinen MR, Alanne AL, et al. Controlling of N-alkyl-polyamine analogue metabolism by selective deuteration. *Biochem J* 2018;475:663–76.
67. Takao K, Shirahata A, Samejima K, et al. Pentamines as substrate for human spermine oxidase. *Biol Pharm Bull* 2013;36:407–11.
68. Goodwin AC, Shields CED, Wu S, et al. Polyamine catabolism contributes to enterotoxigenic *Bacteroides fragilis*-induced colon tumorigenesis. *Proc Natl Acad Sci USA* 2011;108:15354–9.
69. Chaturvedi R, de Sablet T, Asim M, et al. Increased *Helicobacter pylori*-associated gastric cancer risk in the Andean region of Colombia is mediated by spermine oxidase. *Oncogene* 2015;34:3429–40.
70. Melchiorre C, Minarini A, Angeli P, et al. Polymethylene tetraamines as muscarinic receptor probes. *Trends Pharmacol Sci* 1989;Suppl:55–9.
71. Zini M, Passariello CL, Gottardi D, et al. Cytotoxicity of methocramine and methocramine-related polyamines. *Chem Biol Interact* 2009;181:409–16.
72. Minarini A, Zini M, Milelli A, et al. Synthetic polyamines activating autophagy: effects on cancer cell death. *Eur J Med Chem* 2013;67:359–66.